

***Ab initio* pressure-dependent vibrational and dielectric properties of CeO₂**

Tanju Gürel and Resul Eryiğit

Department of Physics, Abant İzzet Baysal University, Bolu-14280, Turkey

(Received 27 April 2006; published 20 July 2006)

We have performed an *ab initio* study of pressure-dependent dielectric and lattice dynamical properties of CeO₂. The calculations have been carried out within the local density functional approximation using norm-conserving pseudopotentials and a plane-wave basis. Born effective charge tensors, dielectric permittivity tensors, the phonon dispersion curves, and their Grüneisen parameters are calculated using density functional perturbation theory. The calculated results agree well with the experiments. Also, we have found that treating the 4*f* electrons of cerium as valence states is crucial for a satisfactory description of the lattice dynamical properties of CeO₂.

DOI: [10.1103/PhysRevB.74.014302](https://doi.org/10.1103/PhysRevB.74.014302)

PACS number(s): 78.30.Hv, 62.20.Dc, 77.22.Ch

I. INTRODUCTION

Cerium oxide (CeO₂) or ceria is a rare-earth oxide which has numerous applications in technology. CeO₂ is extensively used in the modern catalytic industry because of its high oxygen storage capability. It is the major component in catalytic converters to reduce harmful emissions from automobile exhausts.¹ The cubic fluorite crystal structure of CeO₂ with a small lattice-constant mismatch to Si (~0.35%) makes it suitable for high-quality epitaxy on silicon to produce silicon-on-insulator structures² and stable buffer layers of high-temperature superconductors in current-carrying applications.³ A CeO₂ layer on silicon, which has a high dielectric constant, is also attractive as a high-storage capacitor.⁴

In spite of its wide technological usage, the lattice dynamical properties of CeO₂ have been investigated only by a small number of experimental and theoretical studies. On the experimental side, the Brillouin zone center (BZC) phonon frequencies have been measured and reported by using infrared (ir) reflectivity⁵⁻⁷ and Raman spectroscopy⁸⁻¹⁴ techniques. The pressure dependence of the Raman- as well as ir-active BZC modes was investigated in Ref. 15. Phonon frequencies along high-symmetry directions of the Brillouin zone have been determined from inelastic neutron scattering experiments by Clausen *et al.*¹⁶ whose reported data contain only the modes with frequencies below 500 cm⁻¹. The hydrostatic pressure dependence of structural properties of CeO₂ were investigated by high-pressure Raman¹⁵ and x-ray diffraction^{17,18} studies and it has been found that bulk CeO₂ has a phase transition from fluorite-type to α -PbCl₂-type structure at about 31 GPa pressure. For nanocrystalline CeO₂ the transition occurs at significantly lower pressures 26.5 (Ref. 19) or 22.3 GPa.²⁰

On the theoretical side, the whole phonon dispersion curves of CeO₂ have been studied by using phenomenological models only.^{9,10,16,21,22} Model calculations have two main drawbacks: the types of interactions that are taken into account might not be enough to account for the binding properties of the solid, and furthermore, the interaction parameters of the model have to be derived from a fit to experimentally measured quantities. This is a major deficiency when the experimental results are incomplete or contradic-

tory. For example, Sato and Tateyama²¹ have employed a rigid-ion model to calculate the phonon dispersion of CeO₂. Their model uses the elastic constants as part of the input parameters, but since those were not available for CeO₂ at that time, Ref. 21 chose to use those of ThO₂ which were in turn found to be quite different from the experimental ones.¹⁰ Also, the LO frequency used in that calculation appears to be much higher than the value found in infrared measurements.^{5,6} Weber *et al.*⁹ also used the rigid-ion model and the elastic constants predicted by their model differ markedly from the experimental values.¹⁰ The only previous *ab initio* study that we are aware of for the lattice dynamical properties of CeO₂ was by Yamamoto *et al.*,²³ who calculated the dielectric constants, Born effective charges, and ir-active TO phonon frequency at the BZC with density functional theory (DFT), the local density approximation (LDA), using ultra-soft pseudopotentials and plane-wave basis sets.

An important reason for the sparseness of first-principles studies on the lattice dynamical properties of ceria has been the difficulty of treating the nature of occupation and bonding of the 4*f* electrons of cerium in a DFT LDA framework. Recent studies of structural properties suggest a valence band picture²⁴ which is also found to be the case for a good description of the lattice dynamical properties. In this study, we looked at lattice dynamical properties and their pressure dependencies for CeO₂. The dispersion curves of phonon frequencies and the mode Grüneisen parameters have been obtained using density functional and density functional perturbation theory. The Born effective charges, dielectric permittivity tensors, and their behavior under pressure have also studied.

This paper is organized as follows. In Sec. II computational details of the work are briefly reviewed. In the following section, the results of our calculations are presented, discussed and compared to experiments. Section IV concludes the paper with a brief review of the main results.

II. COMPUTATIONAL DETAILS

All of the calculations reported here were performed by using the ABINIT implementation²⁵ of density functional theory with a plane-wave basis set for the wave functions and periodic boundary conditions. Cerium oxide has the

TABLE I. Calculated equilibrium lattice parameter (a_0), bulk modulus (B_0), its pressure derivative (B'_0), and elastic constants of CeO₂ compared to other theoretical and experimental data. (a_0 is in Å, B_0 and elastic constants in GPa, and B'_0 dimensionless.) (GGA, generalized gradient approximation; FP LMTO, full-potential linear muffin tin orbital; PP, plane-wave pseudopotential method; PAW, projector-augmented wave method; SIC, self-interaction corrected; LSD, local spin density approximation.)

a_0	B_0	B'_0	C_{11}	C_{12}	C_{44}	Method
5.366	210.1	4.4	386	124	73	This work
5.406	230	4.0				Expt. (Ref. 17)
5.411	236	4.4				Expt. (Ref. 18)
5.411	220	4.4				Expt. (Ref. 37)
	204		403	105	60	Expt. (Ref. 10)
			450	117	57	Shell Model (Ref. 16)
5.421						PP GGA (Ref. 38)
5.405						PP LDA (Ref. 23)
5.39	214.7					FP LMTO (Ref. 24)
5.45	193.5					PAW GGA (Ref. 39)
5.384	176.9					SIC LSD (Ref. 37)

fluorite structure with three atoms per primitive face-centered-cubic cell; Ce is located at (0,0,0) while two oxygens are at $\pm(1/4, 1/4, 1/4)$ reduced positions.

The interaction between the valence electrons and nuclei and core electrons is described by using Hartwigsen-Goedecker-Hutter (HGH) pseudopotentials²⁶ which use the local density approximation to the exchange-correlation functional. A pseudopotential DFT description of cerium is difficult because of questions related to the nature of occupation and bonding of $4f$ electrons as well as the appreciable overlap of $5s$ and $6p$ core orbitals with the valence orbitals. First-principles calculations indicate that $4f$ electron should be treated as valence electron in CeO₂ and as core electrons in hexagonal form of ceria Ce₂O₃.²⁴ We have found that, among a number of pseudopotentials that were tested,^{27–29} the HGH one is the only one that is able to reproduce the lattice dynamical properties with acceptable accuracy. The cerium HGH pseudopotential used in this study treats semi-core $5s$ and $5p$ electrons and as a result require an extremely high kinetic energy cutoff; $E_{\text{cutoff}}=160$ hartrees was found to be adequate for the convergence of the total energy at the 1 meV level.

The Brillouin zone integrations were tested for $4 \times 4 \times 4$ and $8 \times 8 \times 8$ Monkhorst-Pack grids³⁰ and the $4 \times 4 \times 4$ grid was found to be enough for the convergence of elastic as well as dynamical properties.

Lattice dynamical and elastic properties are calculated within the framework of density functional perturbation theory.³¹ Technical details of the computation of responses to strain perturbations, atomic displacements, and homogeneous electric fields can be found in Refs. 32 and 33, while Ref. 34 presents the subsequent computation of dynamical matrices, Born effective charges, dielectric permittivity tensors, and interatomic force constants. The details of the calculation of elastic constants in the linear response framework are given in Ref. 33.

III. RESULTS

A. Atomic structure and lattice properties

The calculated equilibrium lattice parameter (a_0), bulk modulus (B_0), pressure derivative of bulk modulus (B'_0), and elastic stiffness constants of CeO₂ are displayed in Table I along with some data in the literature. The equilibrium lattice parameter a_0 obtained by energy and force minimization has only a discrepancy of 0.8% with the experimental value. The bulk modulus and its pressure derivative are calculated by fitting to a third-order Vinet equation of state.³⁵ Considering the fact that the zero-point motion and thermal effects are not taken into account,³⁶ the calculated B_0 and B'_0 values agree with the experimental values reasonably well.^{10,17,18,37} In the framework of DFT LDA, our calculated values of elastic constants are compatible with the experimental data of Nakajima *et al.*¹⁰ which were obtained from Brillouin scattering measurements.

B. Born effective charges and dielectric constants

For insulators, the Born effective charge is a measure of the change in electronic polarization due to ionic displacements. For atom κ , $Z_{\kappa,\beta\alpha}^*$ quantifies, to linear order, the polarization per unit cell, created along the direction β when the atoms of sublattice κ are displaced along the direction α , under the condition of zero electric field. Computationally, it is the mixed second derivative of the total energy with respect to the macroscopic field component E_α and the β component of the displacement of κ th particle. The form of Z^* for a particular atom depends on the symmetry of the site occupied by that atom. In CeO₂, cerium and oxygens reside at $4a$ and $8c$ Wyckhoff positions, respectively. The point symmetries of these positions are O_h and T_d . So one would expect the effective charge tensor for both atomic species to be isotropic. The Born effective charges of cerium and oxygen are calculated to be $Z_{\text{Ce}}^*=5.5762$ and $Z_{\text{O}}^*=-2.7881$, re-

TABLE II. Calculated static and high-frequency dielectric constants and zone-center infrared-active phonon frequencies (in units of cm^{-1}).

	ϵ_∞	ϵ_0	ω_{TO}	ω_{LO}	Ref.
Calc.	6.23	23.0	301	579	This work
Calc.	7.5	24.3	305		23
Calc.	2.85	16.6			16
Expt.	5.31	≈ 24.5	272	595	5
Expt.	4.7	35.3	218	597	6
Expt.	6	23	283		7

spectively. The calculation for the effective charges is very well converged as can be seen from the satisfaction of the acoustic sum rule ($\sum Z^* = 0$). The calculated values are in close agreement with those calculated by Yamamoto *et al.*²³ ($Z_{\text{Ce}}^* = 5.712$, $Z_{\text{O}}^* = -2.856$) who used a similar pseudopotential plane-wave LDA method.

The pressure dependence of Born effective charges can reveal important information about the bonding structure of the material. The hydrostatic pressure dependence of Z^* can be analyzed by defining a charge Grüneisen parameter γ^* as $\gamma^* = -\frac{d \ln Z^*}{d \ln V}$ where V is the unit-cell volume. The Grüneisen parameters of Born effective charges are found to be 0.37 for both Z_{Ce}^* and Z_{O}^* .

The form of the dielectric tensor is determined by the symmetry of the crystal. Since CeO_2 is a cubic material its electronic (ϵ_∞) and static (ϵ_0) dielectric tensors have only one component. We display our calculated dielectric constants along with theoretical calculations and experimentally available data in Table II. The experimental ϵ_∞ values range from 4.7 (Ref. 6) to 6 (Ref. 7) while our computed value is 6.23. It is well known that DFT LDA calculations overestimate the values of the high-frequency dielectric constant because of the band-gap problem. But also comparing the theoretical ϵ_0 value computed here (23.0) with the infrared data of Ref. 7, we can say that the agreement is excellent, though probably an accidental agreement.

For the pressure dependence of the dielectric constants one can define a Grüneisen parameter as $\gamma^\epsilon = -\frac{d \ln \epsilon}{d \ln V}$. We have found that the Grüneisen parameters for the electronic and static dielectric constants are found to be $\gamma^{\epsilon_\infty} = -0.10$ and $\gamma^{\epsilon_0} = -2.66$, respectively. These numbers indicate that both constants decrease under pressure but the static part is more sensitive to pressure changes.

C. Phonons

CeO_2 has a cubic fluorite-type structure and belongs to the space group $O_h^5 (Fm\bar{3}m)$. It has three atoms per primitive unit cell. The cerium atom is located at (0,0,0) and the two oxygen atoms at $(\pm 0.25, \pm 0.25, \pm 0.25)$. A factor group analysis gives the decomposition of the zone center modes as $2T_{2u} + T_{1g}$. The threefold-degenerate T_{1g} mode is only Raman active while one of the T_{2u} modes is only infrared active; the other threefold-degenerate T_{2u} mode is the acoustical mode. The degeneracy of the optical T_{2u} is partially lifted by the

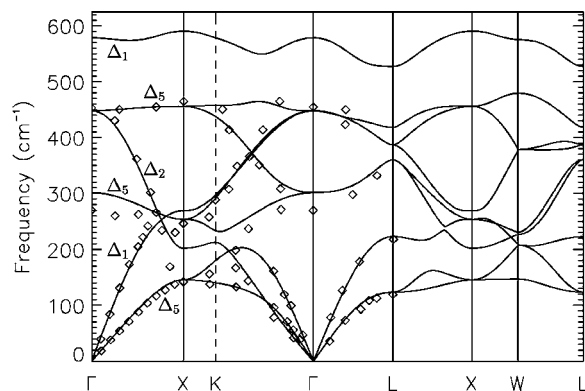


FIG. 1. Calculated phonon dispersions of CeO_2 through high-symmetry points of Brillouin zone with neutron data (diamonds) of Ref. 16.

inclusion of polarization effects, which leads to LO-TO splitting.

Our calculated Γ point phonon frequencies are displayed along with several infrared data in Table II. Before discussing these results, we should point out that an interesting finding from the phonon calculations is the relative insensitivity of zone center phonon mode frequencies to the energy cutoff for the wave functions compared to the convergence of the total energy. The total energy is converged at 1 meV level for $E_{\text{cut}} = 160$ hartrees while the phonon modes seem to converge at a lower cutoff; as part of the convergence study, we have compared the Γ point vibration frequencies for $E_{\text{cut}} = 60, 100,$ and 160 hartrees. While there is a considerable difference between the frequencies calculated at $E_{\text{cut}} = 60$ and 100 hartrees, the difference between those calculated at $E_{\text{cut}} = 100$ and 160 hartrees is less than 0.5%. The agreement between the theoretical results and experimental data is very good for the Raman and the T_{2u} LO modes. The T_{2u} TO mode frequency reported by Ref. 6 seems to be too low compared to the infrared data of Refs. 5 and 7 as well as our calculated result. Compared to the frequency reported in Refs. 5 and 7, our computed T_{2u} TO frequency is $\approx 9\%$ higher. In LDA linear response calculations a difference up to 10% might be expected, but here such a large difference is seen only for one of the modes. A similar overestimation of the TO branch has been encountered in previous *ab initio* pseudopotential calculations of other fluorite structures such as CaF_2 ,^{40,41} PbF_2 ,⁴² BaF_2 ,⁴² and at the Γ point of CeO_2 .²³

The phonon dispersions along the high-symmetry directions were calculated from the interatomic force constants which were obtained from the interpolation of $4 \times 4 \times 4$ (eight irreducible q points) and $8 \times 8 \times 8$ (28 irreducible q points) grids. The overall difference between the frequencies obtained from the two grids is less than 1%. The calculated phonon dispersion relations along the Γ -X-K- Γ -L-X-W-L direction is displayed in Fig. 1 along with the neutron scattering data of Clausen *et al.*¹⁶ The overall agreement between the theoretical results and the experimental data is excellent except for the moderate disagreement mentioned in the previous paragraph. The disagreement for the T_{2u} TO branch, which is $\approx 9\%$ around the BZ center, decreases toward the zone boundary points (X and L). Another observation from

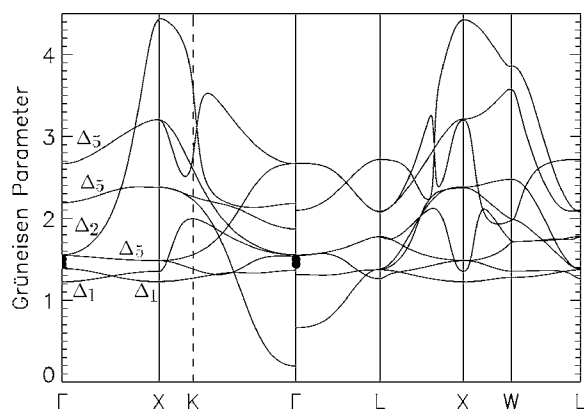


FIG. 2. Calculated mode Grüneisen parameters of CeO₂ through high-symmetry points of the Brillouin zone. Closed circles at the Γ point are the experimental results of Ref. 15.

Fig. 1 is the near-dispersionless character of the LO mode which is also found in other fluorite structures.^{40–42}

D. Mode Grüneisen parameters

The volume dependence of the phonon frequencies can be characterized by the mode Grüneisen parameters

$$\gamma_i(\mathbf{q}) = - \frac{d \ln \omega_i(\mathbf{q})}{d \ln V},$$

where $\omega_i(\mathbf{q})$ is the frequency of the mode i at wave vector \mathbf{q} of BZ and V is the unit cell volume of the crystal. Figure 2 presents the dispersion of the mode Grüneisen parameters along the high-symmetry directions of the BZ. As can be seen from the figure, γ_i ranges mostly from 1 to 3 and all are positive, which indicates that all mode frequencies increase with increasing pressure. The experimental mode Grüneisen parameters of CeO₂ are available only for the zone center modes. Kourouklis *et al.*¹⁵ have calculated the mode Grüneisen parameters of the Raman mode ($\gamma_R=1.44$) and infra-

red mode ($\gamma_{\text{irLO}}=1.5$) of CeO₂ at the zone center by using their experimental $d\omega/dP$ and bulk modulus B value from the relationship $\gamma=(B/\omega_0)(d\omega/dP)$. Our calculated zone center mode Grüneisen parameters for T_{1g} and T_{2u} LO modes are $\gamma=1.55$ and 1.39, respectively, which show a reasonably good agreement with the data reported by Ref. 15.

IV. CONCLUSION

We have presented the results of first-principles calculations on structural, elastic, dielectric, and lattice dynamical properties of CeO₂. The Born effective charges, dielectric constants and phonon dispersion curves have been calculated by using density functional perturbation theory. The pressure dependence of these quantities has also been investigated by the determination of the proper Grüneisen parameters. Our results indicate that for a proper description of these quantities one needs to take into account the semicore states of cerium and treat the $4f$ electrons of cerium as valence electrons. We have found a surprisingly good agreement between the calculated and experimental dielectric constant using HGH pseudopotentials that possess the mentioned electronic properties. The calculated phonon dispersion curves are found to be in good agreement, in magnitude as well as in shape, with the neutron data throughout the high-symmetry directions of the Brillouin zone except for a slight overestimation of the frequency of this branch is a typical behavior in the fluorite-type materials. From the calculation of the hydrostatic pressure dependence of the phonon frequencies, we have found that all the modes have positive Grüneisen parameters, which indicates that mode frequencies increase with increasing pressure.

ACKNOWLEDGMENTS

This work was supported by Tübitak under Grant No. TBAG-2449(104T057) and AIBU Research Fund Grant No. 04.03.02.199.

¹M. S. Dresselhaus and I. L. Thomas, *Nature (London)* **414**, 332 (2001).

²T. Inoue, Y. Yamamoto, S. Koyama, S. Suzuki, and Y. Ueda, *Appl. Phys. Lett.* **56**, 1332 (1990).

³Li Luo, X. D. Wu, R. C. Dye, R. E. Muenchausen, S. R. Foltyn, Y. Coulter, C. J. Maggiore, and T. Inoue, *Appl. Phys. Lett.* **59**, 2043 (1991).

⁴Y. Nishikawa, N. Fukushima, N. Yasuda, K. Nakayama, and S. Ikegawa, *Jpn. J. Appl. Phys., Part 1* **41**, 2480 (2002).

⁵S. Mochizuki, *Phys. Status Solidi B* **114**, 189 (1982).

⁶F. Marabelli and P. Wachter, *Phys. Rev. B* **36**, 1238 (1987).

⁷N. I. Santha, M. T. Sebastian, P. Mohanan, N. M. Alford, K. Sarma, R. C. Pullar, S. Kamba, A. Pashkin, P. Samukhina, and J. Petzelt, *J. Am. Ceram. Soc.* **87**, 1233 (2004).

⁸V. G. Keramidis and W. B. White, *J. Chem. Phys.* **59**, 1561 (1973).

⁹W. H. Weber, K. C. Hass, and J. R. McBride, *Phys. Rev. B* **48**, 178 (1993).

¹⁰A. Nakajima, A. Yoshihara, and M. Ishigame, *Phys. Rev. B* **50**, 13297 (1994).

¹¹S. Kanakaraju, S. Mohan, and A. K. Sood, *Thin Solid Films* **305**, 191 (1997).

¹²J. E. Spanier, R. D. Robinson, F. Zhang, S.-W. Chan, and I. P. Herman, *Phys. Rev. B* **64**, 245407 (2001).

¹³S. Wang, W. Wang, J. Zuo, and Y. Qian, *Mater. Chem. Phys.* **68**, 246 (2001).

¹⁴I. Kosacki, T. Suzuki, H. U. Anderson, and P. Colomban, *Solid State Ionics* **149**, 99 (2002).

¹⁵G. A. Kourouklis, A. Jayaraman, and G. P. Espinosa, *Phys. Rev. B* **37**, 4250 (1988).

¹⁶K. Clausen, W. Hayes, J. E. Macdonald, R. Osborn, P. G. Schnabel, M. T. Hutchings, and A. Magerl, *J. Chem. Soc., Faraday*

- Trans. 2 **83**, 1109 (1987).
- ¹⁷S. J. Duclos, Y. K. Vohra, A. L. Ruoff, A. Jayaraman, and G. P. Espinosa, Phys. Rev. B **38**, 7755 (1988).
- ¹⁸L. Gerward and J. S. Olsen, Powder Diffr. **8**, 127 (1993).
- ¹⁹S. Rekhi, S. K. Saxena, and P. Lazor, J. Appl. Phys. **89**, 2968 (2001).
- ²⁰Z. Wang, S. K. Saxena, V. Pischedda, H. P. Liermann, and C. S. Zha, Phys. Rev. B **64**, 012102 (2001).
- ²¹T. Sato and S. Tateyama, Phys. Rev. B **26**, 2257 (1982).
- ²²M. M. Sinha, P. Ashdhir, H. C. Gupta, and B. B. Tripathi, Phys. Status Solidi B **191**, 101 (1995).
- ²³T. Yamamoto, H. Momida, T. Hamada, T. Uda, and T. Ohno, Thin Solid Films **486**, 136 (2005).
- ²⁴N. V. Skorodumova, R. Ahuja, S. I. Simak, I. A. Abrikosov, B. Johansson, and B. I. Lundqvist, Phys. Rev. B **64**, 115108 (2001).
- ²⁵X. Gonze, J.-M. Beuken, R. Caracas, F. Detraux, M. Fuchs, G.-M. Rignanese, L. Sindic, M. Verstraete, G. Zerah, F. Jollet, M. Torrent, A. Roy, M. Mikami, Ph. Ghosez, J.-Y. Raty, and D. C. Allan, Comput. Mater. Sci. **25**, 478 (2002); <http://www.abinit.org>
- ²⁶C. Hartwigsen, S. Goedecker, and J. Hutter, Phys. Rev. B **58**, 3641 (1998).
- ²⁷We have tested Trouillier-Martins type norm-conserving pseudopotentials (PSPNC) and its Fritz Haber Institute (FHI) variants. Although the lattice constants were found to be in reasonable agreement with the experimental values, the calculated bulk modulus was more than $\approx 30\%$ higher than the experimental one.
- ²⁸The actual PSPNC pseudopotential files used are available at www.abinit.org/Psps/?text=../Psps/LDA_TM/lda
- ²⁹The actual FHI pseudopotential files used are available at www.abinit.org/Psps/?text=../Psps/LDA_FHI/fhi
- ³⁰H. J. Monkhorst and J. D. Pack, Phys. Rev. B **13**, 5188 (1976).
- ³¹S. Baroni, S. de Gironcoli, A. Dal Corso, and P. Giannozzi, Rev. Mod. Phys. **73**, 515 (2001).
- ³²X. Gonze, Phys. Rev. B **55**, 10337 (1997).
- ³³D. R. Hamann, X. Wu, K. M. Rabe, and D. Vanderbilt, Phys. Rev. B **71**, 035117 (2005).
- ³⁴X. Gonze and C. Lee, Phys. Rev. B **55**, 10355 (1997).
- ³⁵P. Vinet, J. H. Rose, J. Ferrante, and J. R. Smith, J. Phys.: Condens. Matter **1**, 1941 (1989).
- ³⁶R. Gaudoin and W. M. C. Foulkes, Phys. Rev. B **66**, 052104 (2002).
- ³⁷L. Gerward, J. S. Olsen, L. Petit, G. Vaitheeswaran, V. Kanchana, and A. Svane, J. Alloys Compd. **400**, 56 (2005).
- ³⁸C. J. Pickard, B. Winkler, R. K. Chen, M. C. Payne, M. H. Lee, J. S. Lin, J. A. White, V. Milman, and D. Vanderbilt, Phys. Rev. Lett. **85**, 5122 (2000).
- ³⁹Z. Yang, T. K. Woo, M. Baudin, and K. Hermansson, J. Chem. Phys. **120**, 7741 (2004).
- ⁴⁰M. Verstraete and X. Gonze, Phys. Rev. B **68**, 195123 (2003).
- ⁴¹K. Schmalzl, D. Strauch, and H. Schober, Phys. Rev. B **68**, 144301 (2003).
- ⁴²A. Dubinin, B. Winkler, K. Knorr, and V. Milman, Eur. J. Biochem. **39**, 27 (2004).